Open Journal of Applied Sciences, 2023, 13, 2141-2148
https://www.scirp.org/journal/ojapps
ISSN Online: 2165-3925
ISSN Print: 2165-3917

Research on Well Testing Interpretation of Low Permeability Deformed Dual Medium Reservoir

Meinan Wang, Yue Xie, Rui Zhang, Guohao Zhang, Jianguo Liu

Bohai Oilfield Research Institute of CNOOC Ltd.-Tianjin Branch, Tianjin, China
Email: wangmn2@cnooc.com.cn

How to cite this paper: Wang, M.N., Xie, Y., Zhang, R., Zhang, G.H. and Liu, J.G. (2023) Research on Well Testing Interpretation of Low Permeability Deformed Dual Medium Reservoir. *Open Journal of Applied Sciences*, **13**, 2141-2148.
https://doi.org/10.4236/ojapps.2023.1311166

Received: October 30, 2023
Accepted: November 26, 2023
Published: November 29, 2023

Abstract

Considering the influence of quadratic gradient term and medium deformation on the seepage equation, a well testing interpretation model for low permeability and deformation dual medium reservoirs was derived and established. The difference method was used to solve the problem, and pressure and pressure derivative double logarithmic curves were drawn to analyze the seepage law. The research results indicate that the influence of starting pressure gradient and medium deformation on the pressure characteristic curve is mainly manifested in the middle and late stages. The larger the value, the more obvious the upward warping of the pressure and pressure derivative curve; the parameter characterizing the dual medium is the crossflow coefficient. The channeling coefficient determines the time and location of the appearance of the "concave". The smaller the value, the later the appearance of the "concave", and the more to the right of the "concave".

Keywords

Low Permeability Oil Reservoirs, Deformation Medium, Dual Media, Cross Flow Coefficient, Well Testing Interpretation Model

1. Introduction

The development of low permeability oil fields is closely related to fractures. Compared with conventional oil reservoirs, the flow patterns in fractures and matrices in low permeability fractured oil reservoirs are complex and variable. How to calculate, predict, and analyze the productivity dynamics of fractures and matrices is an important task in the development of low permeability oil fields [1] [2] [3] [4] [5]. A large number of indoor experiments and field development have shown [6] [7] [8] [9] [10] that, the flow of low permeability reservoirs must overcome a certain threshold pressure gradient in order to flow. Secondly, in the development of low permeability reservoirs, it is necessary to consider the impact of medium deformation on permeability. Low permeability deformation dual medium reservoirs have dual pore characteristics, and there is a phenomenon of crossflow between pores and matrix [11] [12] [13] [14] [15]. In order to effectively characterize the percolation characteristics of low permeability deformation dual media and improve the interpretation level of well testing in such reservoirs, this article comprehensively considers the effects of starting pressure gradient, quadratic gradient term, dual pore characteristics of fractured reservoirs, and medium deformation, and deduces a well testing interpretation model for low permeability dual medium reservoirs, analyzing the seepage law of fractured low permeability reservoirs.

2. Establishment and Solution of Well Testing Interpretation Model for Low Permeability Deformed Dual Medium Reservoir

Assumption: 1) The fluid is slightly compressible. 2) Neglecting the influence of gravity and capillary force. 3) Oil wells are produced at a constant production rate q, with consistent reservoir thickness. 4) The flow through the wellbore is through cracks, with rock blocks as the source. 5) The porosity of each medium is independent of the pressure change of another medium. 6) The fluid flow is a single-phase laminar flow. 7) The oil reservoir is homogeneous and isotropic, and extends infinitely horizontally, with the top and bottom boundaries closed. 8) The medium is slightly compressible and the compression coefficient is constant, but its compression can cause significant changes in formation permeability. 9) Using a fracture system and a bedrock system to simulate the dual medium of a fractured reservoir, it is assumed that fluid flows from the bedrock towards the fracture and ultimately into the wellbore.

Considering the flow of single-phase fluid in porous media, the continuity equation for radial flow can be obtained from the principle of mass conservation.

Continuity equation of crack system:

$$-\frac{1}{r}\cdot\frac{\partial}{\partial r}\left(\rho r v_{\mathrm{r}}\right)+q^{*}=\frac{\partial}{\partial t}\left(\varphi_{\mathrm{f}}\rho\right) \tag{1}$$

Continuity equation of bedrock system:

$$-q^{*}=\frac{\partial}{\partial t}\left(\varphi_{\mathrm{m}}\rho\right) \tag{2}$$

Cross flow equation:

$$q^{*}=\frac{\alpha\rho K_{\mathrm{m}}}{\mu}\left(p_{\mathrm{m}}-p_{f}\right) \tag{3}$$

For low permeability reservoirs, fluid flow needs to overcome the starting pressure gradient. Therefore, in order to fully reflect the role of starting pressure, the following method is selected to describe the fluid flow process:

$$\begin{cases} v = 0, \dfrac{\partial p}{\partial r} \le G \\ v = \dfrac{K}{\mu}\left(\dfrac{\partial p}{\partial r} - G\right), \dfrac{\partial p}{\partial r} > G \end{cases} \tag{4}$$

Substitute the motion equation and the flow equation into the continuity equations of the fracture system and the bedrock system respectively, and assume that $\gamma \gg C_{\mathrm{Lf}}$ obtains the flow equation:

$$\frac{\partial^2 p_{\mathrm{f}}}{\partial r^2} + \gamma\left(\frac{\partial p_{\mathrm{f}}}{\partial r}\right)^2 + \left[\frac{1}{r} - \gamma \cdot G\right] \cdot \frac{\partial p_f}{\partial r} - \frac{G}{r} = \frac{\mu}{K_{\mathrm{f}}}\left(\phi_{\mathrm{f}} C_{\mathrm{t1}} \frac{\partial p_{\mathrm{f}}}{\partial t} + \phi_{\mathrm{m}} C_{\mathrm{t2}} \frac{\partial p_{\mathrm{m}}}{\partial t}\right) \tag{5}$$

$$\varphi_{\mathrm{m}} C_{\mathrm{t2}} \frac{\partial p_{\mathrm{m}}}{\partial t} = \frac{\alpha K_{\mathrm{m}}}{\mu}\left(p_{\mathrm{f}} - p_{\mathrm{m}}\right) \tag{6}$$

$$C_{\mathrm{Lf}} = \frac{1}{\rho}\frac{\partial \rho}{\partial p_{\mathrm{f}}}, \quad C_{\mathrm{Lm}} = \frac{1}{\rho}\frac{\partial \rho}{\partial p_{\mathrm{m}}}, \quad C_{\varphi\mathrm{f}} = \frac{1}{\varphi_{\mathrm{f}}}\frac{\partial \varphi_{\mathrm{f}}}{\partial p_{\mathrm{f}}},$$

$$C_{\varphi\mathrm{m}} = \frac{1}{\varphi_{\mathrm{m}}}\frac{\partial \varphi_{\mathrm{m}}}{\partial p_{\mathrm{m}}}, \quad C_{\mathrm{t1}} = C_{\varphi\mathrm{f}} + C_{\mathrm{Lf}}, \quad C_{\mathrm{t2}} = C_{\varphi\mathrm{m}} + C_{\mathrm{Lm}}.$$

The dimensionless mathematical model obtains the dimensionless flow equation:

$$\frac{\partial^2 p_{\mathrm{Df}}}{\partial r_{\mathrm{D}}^2} - \beta\left(\frac{\partial p_{\mathrm{Df}}}{\partial r_{\mathrm{D}}}\right)^2 + \left(\frac{1}{r_{\mathrm{D}}} - B\beta\right)\frac{\partial p_{\mathrm{Df}}}{\partial t_{\mathrm{D}}} + \frac{B}{r_{\mathrm{D}}} = \omega\frac{\partial p_{\mathrm{Df}}}{\partial t_{\mathrm{D}}} + (1-\omega)\frac{\partial p_{\mathrm{Dm}}}{\partial t_{\mathrm{D}}} \tag{7}$$

$$(1-w)\frac{\partial p_{\mathrm{Dm}}}{\partial t_{\mathrm{D}}} = \lambda\left(p_{\mathrm{Df}} - p_{\mathrm{Dm}}\right) \tag{8}$$

$$p_{\mathrm{Df}} = \frac{2\pi h K_0}{\mu q}\left(p_0 - p_{\mathrm{f}}\right), \quad p_{\mathrm{Dm}} = \frac{2\pi h K_0}{\mu q}\left(p_0 - p_{\mathrm{m}}\right),$$

$$r_{\mathrm{D}} = \frac{r}{r_{\mathrm{w}}}, \quad \lambda = \frac{K_{\mathrm{m}} r_{\mathrm{w}}^2}{K_{\mathrm{f}}}\alpha, \quad t_{\mathrm{D}} = \frac{tK_0}{\mu\left(\varphi_{\mathrm{f}} C_{\mathrm{t1}} + \varphi_{\mathrm{m}} C_{\mathrm{t2}}\right) r_{\mathrm{w}}^2},$$

$$\beta = C_\rho\left(p_{\mathrm{i}} - p_{\mathrm{w}}\right), \quad \gamma_{\mathrm{D}} = \frac{\mu q \gamma}{2\pi h K_0}, \quad B = \frac{2\pi h K_0}{\mu q} G, \quad \omega = \frac{\varphi_{\mathrm{f}} C_{\mathrm{t1}}}{\varphi_{\mathrm{f}} C_{\mathrm{t1}} + \phi_{\mathrm{m}} C_{\mathrm{t2}}}$$

The obtained model contains a quadratic gradient term, which can be addressed using Laplace transform.

$$p_{\mathrm{Df}} = -\frac{1}{\beta}\mathrm{In}\left[1 - \beta\eta\left(r_{\mathrm{D}}, t_{\mathrm{D}}\right)\right], \quad p_{\mathrm{Dm}} = \xi\left(r_{\mathrm{D}}, t_{\mathrm{D}}\right), \quad x = \mathrm{In}\, r_{\mathrm{D}} \tag{9}$$

The transformed flow equation is:

$$\frac{\partial^2 \eta}{\partial x^2} - B\beta \mathrm{e}^x \frac{\partial \eta}{\partial x} + \mathrm{e}^x B(1-\beta\eta) = \omega \mathrm{e}^{2x}\frac{\partial \eta}{\partial t_{\mathrm{D}}} + (1-\omega)\mathrm{e}^{2x}(1-\beta\eta)\frac{\partial \xi}{\partial t_{\mathrm{D}}} \tag{10}$$

$$(1-\omega)\frac{\partial \xi}{\partial \Delta t_{\mathrm{D}}} = \lambda\left[-\frac{1}{\beta}\mathrm{In}(1-\beta\eta) - \xi\right] \tag{11}$$

After transformation, the quadratic gradient term is absorbed into the equation without any approximation, and the coefficients of the nonlinear term of the equation are only limited to the right side of the equation.

Using an implicit difference scheme to obtain the numerical solution of the model, *i.e.* using $\eta(x, t_D)$ and $\xi(x, t_D)$ Write the difference schemes for Equations (10) and (11) regarding the first-order backward difference quotient of t_D and the second-order difference quotient of x:

$$\begin{aligned}&\frac{\eta_{i+1}^{n+1}-2\eta_i^{n+1}+\eta_{i-1}^{n+1}}{\Delta x^2}-B\beta e^{i\cdot\Delta x}\frac{\eta_{i+1}^{n+1}-\eta_i^{n+1}}{\Delta x}+Be^{i\cdot\Delta x}\left(1-\beta\eta_i^{n+1}\right)\\&=\omega e^{2i\cdot\Delta x}\frac{\eta_{i+1}^{n+1}-\eta_i^{n}}{\Delta t_D}+(1-\omega)e^{2i\cdot\Delta x}\left(1-\beta\eta_i^{n}\right)\frac{\xi_i^{n+1}-\xi_i^{n}}{\Delta t_D}\end{aligned} \tag{12}$$

$$(1-\omega)\frac{\xi_i^{n+1}-\xi_i^{n}}{\Delta t_D}=\lambda\left[-\frac{1}{\beta}\text{In}\left(1-\beta\eta_i^{n}\right)-\xi_i^{n}\right] \tag{13}$$

Organize and simplify:

$$c(i)\eta_{i-1}^{n+1}+a(i)\eta_i^{n+1}+b(i)\eta_{i+1}^{n+1}=d(i) \tag{14}$$

$$\xi_i^{n+1}=e(i)\xi_i^{n}+f(i) \tag{15}$$

$$c(i)=1,\quad a(i)=-2+B\beta e^{i\cdot\Delta x}\Delta x-B\beta e^{i\cdot\Delta x}\Delta x^2-\frac{\omega e^{2i\cdot\Delta x}\Delta x^2}{\Delta t_D},$$

$$b(i)=1-B\beta e^{i\cdot\Delta x}\Delta x,\quad \begin{aligned}d(i)=&\left[-\frac{\omega e^{2i\cdot\Delta x}\Delta x^2}{\Delta t_D}-(1-\omega)\beta e^{2i\cdot\Delta x}\Delta x^2\frac{\xi_i^{n+1}-\xi_i^{n}}{\Delta t_D}\right]\eta_i^{n}\\&+\left[(1-\omega)e^{2i\cdot\Delta x}\Delta x^2\frac{\xi_i^{n+1}-\xi_i^{n}}{\Delta t_D}-e^{i\cdot\Delta x}B\Delta x^2\right]\end{aligned},$$

$$e(i)=1-\frac{\lambda\Delta t_D}{1-\omega},\quad f(i)=-\frac{\lambda\Delta t_D}{\beta(1-\omega)}\text{In}\left(1-\beta\eta_i^{n}\right).$$

Substituting the initial value conditions of the difference scheme into the difference scheme of the flow equation results in an N-order system of tridiagonal equations. At each moment, we can list this coefficient matrix, and then we can use the Thomas algorithm to solve the pressure distribution at the next moment, $n+1$, based on the pressure value of each grid at time n, and so on.

3. Research on Well Testing Interpretation of Low Permeability Dual Deformation Medium Reservoir

Applying the well testing interpretation model established in this article for low permeability dual deformable medium reservoirs, the seepage law under fixed production conditions with closed outer and inner boundaries was studied. The pressure dynamic curve of the deformable medium reservoir system was drawn, and the influence of various parameter changes on the pressure dynamic curve was analyzed.

Figure 1 shows the effect of medium deformation on the pressure dynamic curve. The medium change has little effect on the early stage of the pressure dynamic curve, but has a greater impact on the pressure curve in the middle and later stages. In the middle and later stages of the pressure dynamic curve, the pressure wave gradually propagates towards the boundary, and the larger the permeability modulus, the more affected the reservoir permeability is by pressure. The lower the permeability, the more obvious the upward warping of the pressure and pressure derivative curve. The appearance of "concave" particles that characterize the characteristics of dual media is not significantly related to the deformation of the medium. The double logarithmic curve in the middle and later stages is significantly upward, showing a characteristic reflected by bounded stratigraphic boundaries.

Figure 2 shows the effect of starting pressure gradient on the pressure dynamic curve. The start-up pressure gradient affects the entire flow process, with a relatively small impact in the initial stage. As time increases, the pressure curves diverge from each other, and the impact of the start-up pressure gradient on the pressure becomes increasingly significant. The larger the starting pressure gradient, the greater the resistance that fluid flow needs to overcome, and the more obvious the upward warping of the pressure and pressure derivative curve. The appearance of "concave particles" characterizing the characteristics of dual media is not significantly related to the starting pressure gradient.

Figure 3 shows the effect of the crossflow coefficient on the pressure dynamic curve. From the figure, it can be seen that the channeling coefficient determines the time and location of the appearance of the "concave". The larger the channeling coefficient, the more fluid flows from the matrix to the crack, the more obvious the channeling phenomenon, and the earlier the "concave" appears.

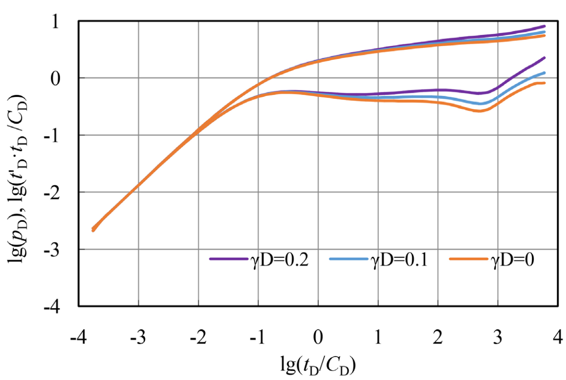

Figure 1. Effect of medium deformation on pressure curve.

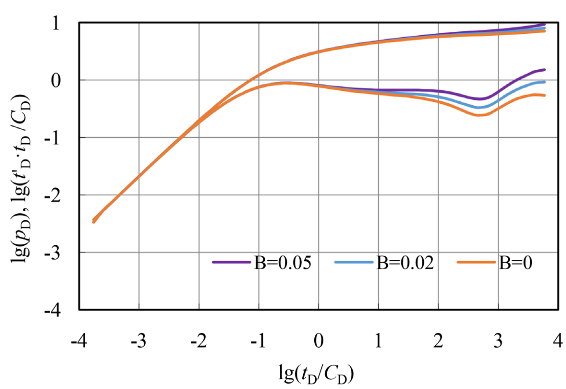

Figure 2. Effect of starting pressure gradient on pressure curve.

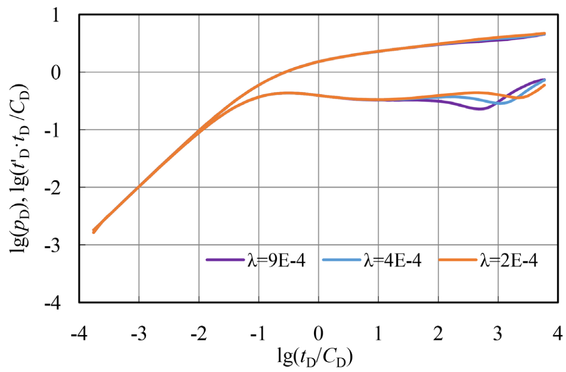

Figure 3. Effect of crossflow coefficient on pressure curve.

4. Conclusions

1) Established a well testing interpretation model for low permeability dual deformation medium reservoirs; taking into account factors such as medium deformation, starting pressure gradient, and quadratic gradient term, a finite difference solution is adopted.

2) The well testing interpretation of low permeability dual deformation medium reservoirs was conducted, and the results showed that the impact of starting pressure gradient and medium deformation on the pressure characteristic curve is mainly manifested in the middle and late stages. The smaller the value, the greater the dimensionless pressure in the later stage, and the faster the pressure in the formation decreases. When both exist simultaneously, the impact will be more significant. The channeling coefficient determines the time and location of the appearance of the "concave". The smaller the value, the later the appearance of the "concave", and the more to the right of the "concave".

Conflicts of Interest

The authors declare no conflicts of interest regarding the publication of this paper.

References

[1] Ji, T.M., Chen, H.M. and Wang, Y.P. (2023) The Inflow Relationship Research of HQ Low Permeability Oil Reservoir. *Petrochemical Industry Application*, **42**, 71-73.

[2] Liu, K., Fan, H.F., Yan, B. and Wu, G.D. (2023) Progress in Mechanism and Technology of Imbibition Recovery in Low Permeability Reservoirs. *Oilfield Chemistry*, **40**, 182-190.

[3] Wang, X.X. (2017) Research on Low Permeability Reservoir Imbibitions Mechanism and Development. *Advances in Fine Petrochemicals*, **18**, 26-29.

[4] Li, C.L., Sun, P.P., Wang, Y.F. and Yang, J.N. (2023) A Calculation Method of Water Breakthrough Time of 5-Point Well Pattern in Low Permeability Reservoir. *Journal of Southwest Petroleum University* (*Science & Technology Edition*), **45**, 67-76.

[5] Sun, N.H., Hou, Y.W., Zhang, D., Wang, W. and Peng, Q. (2020) Productivity Prediction of Horizontal Well under Oil and Gas Two-Phase in Low Permeability Re-

servoirs and Influencing Factors Analysis by Taking Bohai A Oilfield as an Example. *Petroleum Geology and Engineering*, **34**, 74-78.

[6] Wu, M.L., Li, T., Zhao, G.L., Zhao, J.L. and Cai, J.Q. (2022) Well Test Model for Horizontal Well in Dual-Porosity Three-Zone Composite Reservoir. *Well Testing*, **31**, 6-12.

[7] Mao, X.J., Hu, G.W., Zhang, X.W., Zhang, W.Q., Qin, Y.M. and Wang, C.Y. (2021) Simulation Method of Oil-Water Two-Phase Transient Flow in Dual-Porosity System in Tight Reservoir. *Journal of Shenzhen University* (*Science and Engineering*), **38**, 572-578. https://doi.org/10.3724/SP.J.1249.2021.06572

[8] Jiang, R.Z., Gao, Y., Sun, Z.B., Gao, Y.H. and He, S.M. (2020) Bottom Pressure Characteristics for Eccentric Fracture Vertical Well in Dual-Medium Low-Permeability Reservoir. *Fault-Block Oil & Gas Field*, **27**, 778-783.

[9] Lin, W., Fan, H.F., Wang, S.J., Yan, L. and Chen, F.L. (2019) Blasingame Curve Analysis of Fractured Horizontal Well in Tight Oil Reservoir. *Petroleum Geology and Recovery Efficiency*, **26**, 122-128.

[10] Jiang, R.Z., Zhang, C.G., Cui, Y.Z., Zhang, W. and Zhang, F.L. (2018) Nonlinear Flow Model of Dual-Medium Fractal Reservoir Considering Pressure Sensitivity. *Fault-Block Oil & Gas Field*, **25**, 612-616.

[11] Shi, X.W., Yang, Z.M., Duan, X.L., Zhang, Y.P., Zhu, G.Y., Xiao, Q.H. and Wang, X.Y. (2018) Study on Similarity Theory of Water Flooding in Low Permeability Carbonate Reservoir. *Petroleum Geology and Recovery Efficiency*, **38**, 127-129.

[12] Xiao, Z.Y., Zhao, Y.L., Zhang, L.H., Ge, F., Yang, Z.D., Liu, X.Y., Zhang, D.X. and Tian, Y. (2023) Capacity of Compact Reservoir Based on Dual Medium Embedded Discrete Crack Model. *Science Technology and Engineering*, **23**, 10780-10790.

[13] Zhu, Z.Q., Wang, Y.P., Meng, Z.Q., Liu, B. and Deng, J.F. (2023) Study on Fine Fracture Characterization and Percolation Mechanism of Fractured Reservoirs. *Unconventional Oil & Gas*, **10**, 121-126.

[14] Zhang, Y.Y., Li, W.D., Cui, G.L. and Li, S.Q. (2012) Well Test Interpretation Model for Dual Media Low Permeability Reservoir. *Journal of Shaanxi University of Science & Technology*, **30**, 65-69.

[15] Mao, X.L., Liu, Y.T., Feng, Y.L., Zheng, W.K. and Liu, S.P. (2018) Re-Recognition of Dual Effective Stresses and the Comprehensive Effect. *Petroleum Science Bulletin*, **3**, 390-398.

Sign Annotation

r—distance from the well, m;

ρ—density, g/cm^3;

v—Seepage velocity, cm/s;

φ_f— fracture porosity, %;

φ_m—matrix porosity, %;

K_f—fracture Permeability, 10^{-3} μm^2;

K_m—matrix Permeability, 10^{-3} μm^2;

q^*—channeling flow, 10^{-3} μm^2;

p_f—fracture pressure, MPa;

p_f—matrix pressure, MPa;

α—channeling coefficient, f;

C_ρ—liquid compressibility, MPa^{-1};

C_Φ—rock compressibility, MPa^{-1};

C_t —total compressibility, MPa^{-1};

G—Starting pressure gradient, MPa/m;

γ—permeability modulus, MPa^{-1};

h—reservoir thickness, m;

r_w—radius of the well, m;

r_e—drainage radius, m;

L—Length of model, cm;

Δp—Pressure difference, MPa;

η—pseudo pressure, f;.

P_{Df}, P_{Dm} —dimensionless pressure, dimensionless;

r_D—dimensionless radius, dimensionless;

λ—dimensionless channeling coefficient, dimensionless;

t_D—dimensionless time, dimensionless;

β—dimensionless fluid compressibility, dimensionless;

γ_D—dimensionless permeability modulus, dimensionless;

B—dimensionless starting pressure gradient, dimensionless;

ω—dimensionless elastic storage ratio, dimensionless;

ζ—Laplace variable, dimensionless.